

Journal of Materials Chemistry B

Materials for biology and medicine

Accepted Manuscript

This article can be cited before page numbers have been issued, to do this please use: F. Fan, L. Zhang, X. Zhou, F. Mu and G. Shi, *J. Mater. Chem. B*, 2020, DOI: 10.1039/D0TB02269A.



This is an Accepted Manuscript, which has been through the Royal Society of Chemistry peer review process and has been accepted for publication.

Accepted Manuscripts are published online shortly after acceptance, before technical editing, formatting and proof reading. Using this free service, authors can make their results available to the community, in citable form, before we publish the edited article. We will replace this Accepted Manuscript with the edited and formatted Advance Article as soon as it is available.

You can find more information about Accepted Manuscripts in the [Information for Authors](#).

Please note that technical editing may introduce minor changes to the text and/or graphics, which may alter content. The journal's standard [Terms & Conditions](#) and the [Ethical guidelines](#) still apply. In no event shall the Royal Society of Chemistry be held responsible for any errors or omissions in this Accepted Manuscript or any consequences arising from the use of any information it contains.

ARTICLE

A sensitive fluorescent probe for β -galactosidase activity detection and application in ovarian tumors imaging

Fang Fan, Li Zhang, Xinguang Zhou, Fangya Mu and Guoyue Shi*

Received 00th January 20xx,
Accepted 00th January 20xx

DOI: 10.1039/x0xx00000x

The development of non-invasive and sensitive optical probes for in vivo bioimaging of cancer-related enzymes is desirable for early diagnosis and effective cancer therapy. β -galactosidase (β -gal) is regarded as a key ovarian cancer biomarker, owing to its overexpression in primary ovarian cancer. Herein, we designed a sensitive near-infrared (NIR) probe (DCMCA- β gal) for the detection and real-time imaging of β -gal activity in ovarian tumors, thereby achieving the visualization of ovarian tumors by β -gal activity detection. DCMCA- β gal could be triggered by β -gal, resulting in the release of a NIR chromophore DCM-NH₂; the linear range of fluorescent response to β -gal concentration was 0–1.2 U with a low detection limit of 1.26×10^{-3} U mL⁻¹. We used DCMCA- β gal to detect and visualize β -gal activity in SKOV3 human ovarian cancer cells, as well as for real-time imaging of β -gal activity in ovarian cancer mouse models. DCMCA- β gal possessed high sensitivity, “turn-on” NIR emission, a large spectral shift, and high photostability in a dynamic living system and thus could serve as a more sensitive sensor for real-time tracking of β -gal activity in vivo and ovarian tumors imaging.

Introduction

Early accurate diagnostics and effective therapy have great significance in improving cancer survival rates. Ovarian cancer is the leading cause of cancer-associated death in women, with a five-year survival rate < 50%. This high mortality rate is often attributed to delayed diagnosis; approximately 75% of patients with ovarian cancer are diagnosed in later stages [1, 2]. Therefore, early diagnosis is crucial for improving survival; however, the early diagnosis of ovarian cancer is hindered by the lack of obvious symptoms.

Biomarkers are synthesized or released from cells during cancer onset; hence, accurate biomarker detection and activity monitoring in living systems can be utilized for early stage cancer diagnosis, further promoting effective treatment [3]. β -galactosidase (β -gal), with overexpression in primary ovarian cancer, is considered an important biomarker of ovarian cancers [4–6]. Therefore, developing an accurate and fast method for in situ detection and real-time monitoring of β -gal activity is desirable for early diagnosis of ovarian cancer [7, 8].

Non-invasive optical imaging has recently developed to be an ideal tool for tracking enzyme activity in situ [9–14]. Up to now, several optical probes for detecting and visualizing β -gal activity in living systems have been designed and produced [15–29]. Compared with traditional probes, near infrared (NIR) probes demonstrate unique characteristics, such as decreased

auto-fluorescence and deep penetration in tissues, which have proven beneficial for in vivo bioimaging [30–32]; however, highly sensitive NIR probes for imaging ovarian tumors by tracking β -gal activity in vivo are still rare.

Thus, we develop a very sensitive NIR probe for detecting and real-time imaging of β -gal activity in ovarian tumors, and further for visualizing ovarian tumors. Our probe, DCMCA- β gal, utilizes DCM-NH₂ as the NIR fluorescence reporter [33, 34] and β -galactose as the enzyme-activating trigger; these two components are conjugated by a bridge of 4-hydroxy-3-nitrobenzyl alcohol (Scheme 1A). DCMCA- β gal exhibits “turn-on” NIR emission, a large spectral shift, and high photostability under normal physiological conditions; these characteristics make it more suitable for tracking β -gal activity in vivo.

Particularly noteworthy is its high sensitivity for β -gal detection, suggesting that the use of DCMCA- β gal could enable clearer imaging of ovarian tumors and the detection of much smaller metastases. Early reports indicate that the detection and removal of ovarian cancer peritoneal metastases < 1 mm in diameter could improve the five-year survival rate [35, 36]. Therefore, DCMCA- β gal has great potential value for fluorescence-guided diagnosis and therapy of ovarian cancer in preclinical applications.

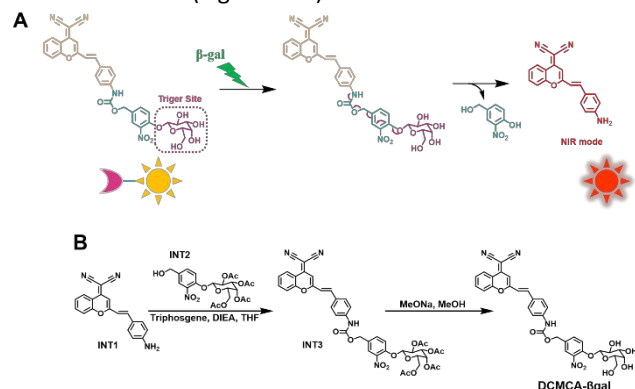
Results and discussion

Design of DCMCA- β gal

In our probe, DCM-NH₂ was used as the NIR fluorescent reporter in terms of its controllable emission, and a β -gal cleavable unit (β -galactose) was used to be the enzyme-activating trigger. These two units were connected by a 4-

^a School of Chemistry and Molecular Engineering, East China Normal University, Dongchuan Road 500, Shanghai 200241, China E-mail: gyshi@chem.ecnu.edu.cn Electronic Supplementary Information (ESI) available: [details of any supplementary information available should be included here]. See DOI: 10.1039/x0xx00000x

hydroxy-3-nitrobenzyl bridge, which could enhance the pull-electron effect in the molecule, thus facilitating the cleavage of the C-O bond between the bridge and trigger site by β -gal, thereby improving the response rate and sensitivity of the probe. This feature was confirmed in subsequent experiments. DCMCA- β gal and other intermediates were characterized by $^1\text{H-NMR}$ and HR-MS (Figs. S1–S8).



Scheme 1 (A) The DCMCA- β gal fluorescent probe for β -gal detection. (B) DCMCA- β gal synthesis process.

DCMCA- β gal response to β -gal in vitro

To assess whether DCMCA- β gal can actually detect β -gal, we studied the optical characteristics of DCMCA- β gal in reaction with β -gal in a physiological buffer solution. Fig. 1A showed that DCMCA- β gal exhibited robust absorption at 452 nm. Following the addition of β -gal, the absorption at 452 nm decreased, while a new red-shifted band at approximately 526 nm appeared. This new absorption pattern was identical to the absorption of DCM-NH₂, demonstrating DCM-NH₂ production following cleavage of the β -galactose unit by β -gal. Additionally, an alteration in color from pale yellow to light red was detected in the test solution.

In terms of the fluorescence response, an obvious ratiometric fluorescent signal ($I_{676\text{ nm}}/I_{550\text{ nm}}$) was observed following β -gal addition (Fig. 1B). The fluorescence intensity (FL intensity) decreased at 550 nm, but drastically increased in the 600–800 nm range, especially at 676 nm. This new and unique red-shifted response was attributed to the liberation of amidogen following β -gal-catalyzed DCMCA- β gal hydrolysis. The formed amino group was a stronger electron donor, which could enhance the intramolecular charge transfer (ICT) and create the NIR emission of DCM-NH₂.

Then the FL intensity ($I_{676\text{ nm}}$) as a function of time was measured. As presented in Fig. 1E, the FL intensity at $I_{676\text{ nm}}$ plateaued in 30 min after β -gal (1.2 U) was added to the DCMCA- β gal solution, with an approximate 12-fold enhancement detected. These results indicated that this rapid response was available for rapid detection of β -gal, and that 30 min was selected as the optimal detection time in subsequent tests.

Following fluorescence titration with β -gal, 5 μM of DCMCA- β gal was chosen as the optimal concentration in terms of

sensitivity and accuracy (Fig. S9). As shown in Figs. 1C and 1D, a good linear relationship was observed between $I_{676\text{ nm}}/I_{550\text{ nm}}$ and β -gal concentration, ranging from 0 to 1.2 U, and the $I_{676\text{ nm}}/I_{550\text{ nm}}$ ratio demonstrated an approximate 19-fold increase. These results demonstrated the high sensitivity of DCMCA- β gal, a low detection limit (D_L) of $1.26 \times 10^{-3}\text{ U mL}^{-1}$ was achieved ($S/N = 3$).

The selectivity of DCMCA- β gal for β -gal was evaluated using common biomolecules and several enzymes. As illustrated in Fig. 1F, no obvious changes in FL intensity ($I_{676\text{ nm}}$) were detected following the addition of 100 equiv. of the interferents. Only after β -gal (1.2 U) was added, was a distinct enhancement in FL intensity ($I_{676\text{ nm}}$) detected, indicating that DCMCA- β gal could be selectively hydrolyzed by β -gal. Consequently, DCMCA- β gal could be employed as a β -gal detection sensor with high sensitivity and selectivity.

In addition, the pH dependence of the DCMCA- β gal (5 μM) was also investigated (Fig. S10). DCMCA- β gal was stable within a pH range of 5 to 10, suggesting that β -gal could be detected in dynamic living systems using DCMCA- β gal without pH interference.

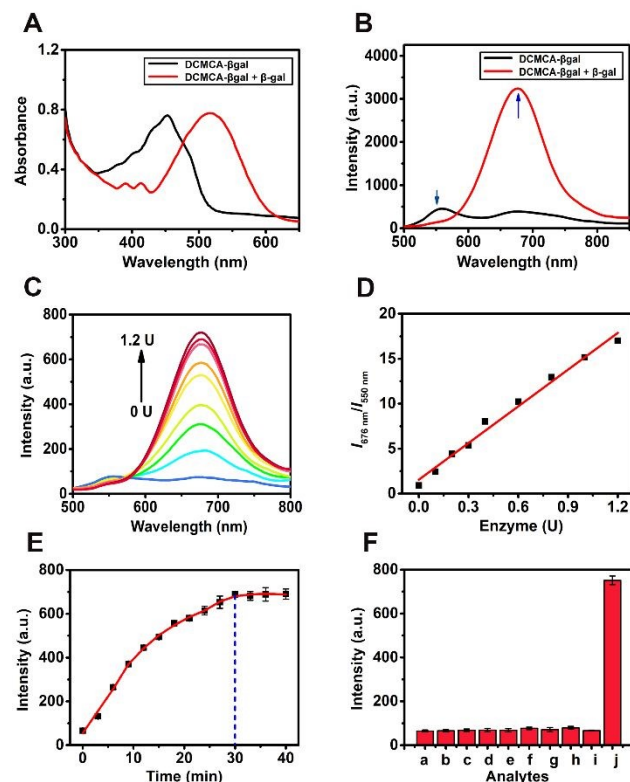


Fig. 1 (A–B) The optical spectra of DCMCA- β gal with or without the addition of β -gal. (C) Fluorescence emission of DCMCA- β gal (5 μM) incubated with 0–1.2 U of β -gal for 30 min at 37 $^{\circ}\text{C}$ ($\lambda_{\text{exc}} = 464\text{ nm}$). (D) $I_{676\text{ nm}}/I_{550\text{ nm}}$ vs. β -gal concentration plot. (E) Fluorescence time-course study of DCMCA- β gal in reaction with β -gal (1.2 U). (F) FL intensity response of DCMCA- β gal (5 μM) to various interferents (100 equiv.): a) reductase; b) phosphatase; c) cellulase; d) lysozyme; e) GSH; f) H₂O₂; g) cysteine; h) H₂S; i) α -gal; j) β -gal.

Sensing mechanism

To get a further insight into the specific sensing mechanism underlying the response of DCMCA- β gal to β -gal, HPLC

experiments were conducted. As shown in Fig. 2, following the incubation of DCMCA- β gal with β -gal, a new peak appeared with a retention time consistent with the fluorophore DCM-NH₂. These results confirmed that an enzyme-triggered cleavage reaction had occurred and that DCM-NH₂ had formed; the β -glycoside bond was cleaved by β -gal, removing the 4-hydroxy-3-nitrobenzyl bridge, then generating an electron-rich amino group. The enzymatic reaction product DCM-NH₂ produced a clear fluorescent signal in the NIR region.

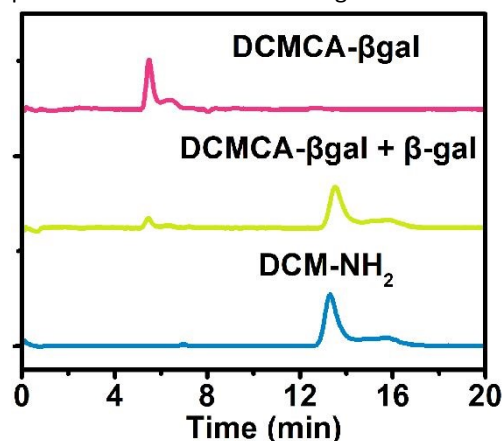


Fig. 2 HPLC traces of DCMCA- β gal, DCMCA- β gal reacted with β -gal, and DCM-NH₂, respectively. HPLC conditions: detection wavelength, 450 nm; eluent solvent, 15% methanol in water with 0.3 mL min⁻¹ flow rate.

Sensing endogenous β -gal in live cells

Subsequently, we evaluated the ability to utilize DCMCA- β gal to monitor and image β -gal activity in live cells using 293T cells as the model. Initially, the lacZ gene was transferred into the 293T cells via facile transfection, resulting in cells (293T/lacZ) harboring endogenous β -gal [37, 38]. Low fluorescence was detected in three specific channels (blue, green, and red channels), when the 293T cells were treated with DCMCA- β gal (5 μ M) at 37 °C for 30 min. In contrast, strong red fluorescence (670 – 800 nm), corresponding to the emission band of DCM-NH₂, was clearly observed in 293T/lacZ cells overexpressing β -gal (Fig. 3B). The mean FL intensity in 293T/lacZ cells was three times greater than that in untreated 293T cells (Fig. S12). Thus, these observations suggested that DCMCA- β gal could image β -gal activity in live cells.

Next, to further confirm the utility of DCMCA- β gal to monitor β -gal activity in live cells, SKOV3 human ovarian cancer cells was proposed. SKOV3 cells have been shown to highly express endogenous β -gal. As presented in Fig. 3E, strong red fluorescence was detected in SKOV3 cells, while no fluorescence was observed in negative control SKOV3 cells pretreated with an inhibitor (Fig. 3H). The mean FL intensity in positive SKOV3 cells increased 25-fold compared with the negative control (Fig. S13). Thus, the results demonstrated that DCMCA- β gal could be triggered by β -gal in cells to release the DCM-NH₂ fluorophore, which provided “turn-on” NIR emission (λ = 676 nm) for monitoring β -gal activity.

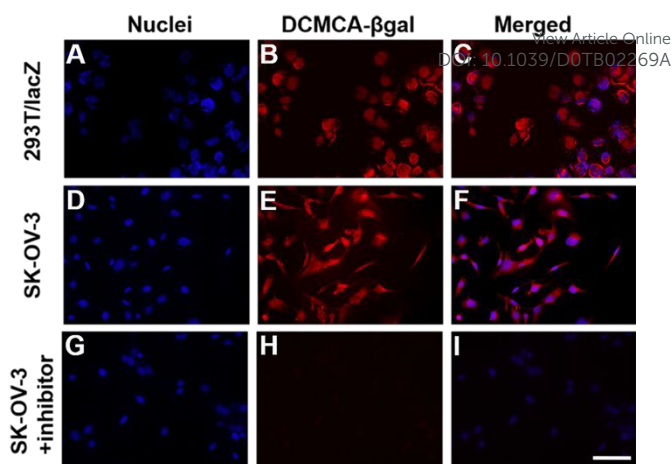


Fig. 3 Fluorescent imaging of DCMCA- β gal incubated with (A – C) 293T/lacZ cells highly expressing β -gal, (D – F) SKOV3 cells, and (G – I) SKOV3 cells following pre-treatment with an inhibitor Scale bar: 50 μ m.

Visualizing β -gal activity in vivo and ovarian tumors imaging

NIR probe possesses unique advantages for in vivo bioimaging, the NIR emission enables to penetrate deep into tissues and avoid interference of auto-fluorescence in vivo. Thus, we designed DCMCA- β gal with “turn-on” NIR emission, and evaluated its ability to visualize β -gal activity in vivo. First, we constructed an ovarian cancer mouse model by subcutaneous inoculation of control 293T and SKOV3 cells into the left and right

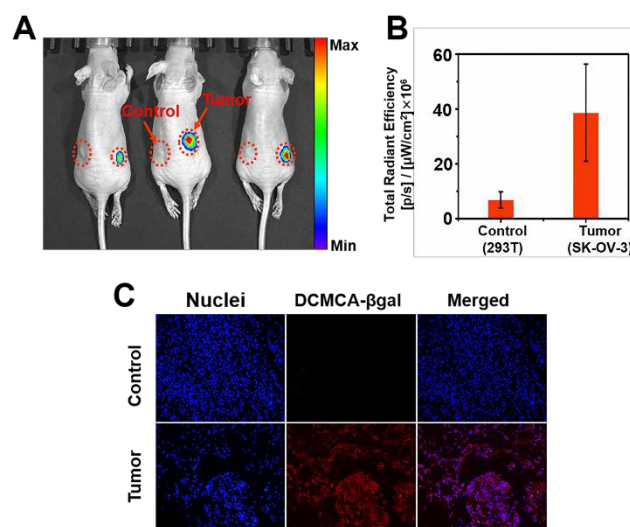


Fig. 4 (A) Fluorescence imaging of DCMCA- β gal in ovarian tumors. DCMCA- β gal was intratumorally injected into tumor-bearing mice; the 293T control tumor is on the left and the SKOV3 tumor is on the right (λ_{exc} = 465 nm). (B) Comparison of fluorescence signals following intratumoral injection of DCMCA- β gal in both flanks. Quantitative analysis was conducted using the IVIS imaging system. (C) Fluorescent images of the dissected tumor tissues.

-t flanks of mice, respectively. As illustrated in Fig. 4A and Fig. S14, 10 min post injection of DCMCA- β gal into the tumors, obvious NIR fluorescence signals ranging from 680 to 720 nm were detected on the right flanks, which gradually increased to

a maximum at 1 h; however, no fluorescence signals were detected on the left flanks, even at 1 h post injection. IVIS imaging system analysis demonstrated that the FL intensity at 680 – 720 nm in tumors on the right flanks was much higher than in the control and a clear description was achieved by quantitative study of the fluorescence images (Fig. 4B). These results showed that DCMCA- β gal could be triggered by β -gal in tumors, releasing the NIR fluorophore to image β -gal activity. Additionally, fluorescence imaging of tumor tissues showed a large increase in NIR fluorescence signals in the ovarian tumors compared with the control (Fig. 4C). The result further confirmed that DCMCA- β gal could be utilized to visualize and track β -gal activity in ovarian tumors, and in turn to image ovarian tumors by β -gal activity detection.

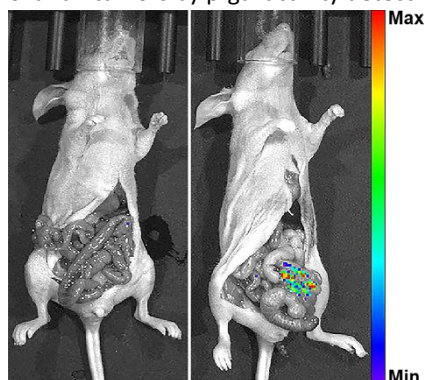


Fig. 5 Fluorescence imaging of DCMCA- β gal in ovarian tumors. DCMCA- β gal was intraperitoneally injected into tumor-bearing mice ($\lambda_{\text{ex}} = 465 \text{ nm}$).

Then, to further confirm the suitability of DCMCA- β gal for ovarian tumors imaging, we built another tumor model of ovarian cancer by intraperitoneal injection of SKOV3 cells into the nude mice. After raised for 10 days, the non-tumor- and tumor-bearing mice were both intraperitoneally injected with the probe DCMCA- β gal. At 40 min post injection, the mice were killed and the abdominal cavities imaging were performed. As displayed in Fig. 5, the NIR fluorescence signals were observed in the tumor-bearing mice and using the signals the ovarian tumors could be clearly visualized, which suggested that DCMCA- β gal had been hydrolyzed by β -gal in the tumors and the NIR fluorophore DCM-NH₂ was released; while no NIR signals was captured in non-tumor-bearing mice. Thus, these results demonstrated the suitability of DCMCA- β gal for ovarian tumors imaging. Additionally, the high sensitivity of DCMCA- β gal enabled the acquisition of much clearer images, which was conducive for the detection of smaller tumor metastases with great significance for improving the the five-year survival rate of patients.

Experimental methods

Reagents and instruments

Malononitrile, 2'-hydroxyacetophenone, sodium hydride (NaH), acetic anhydride, 4-acetamidobenzaldehyde, piperidine, acetobromo- α -D-galactose, 4-hydroxy-3-nitro benzaldehyde, silver oxide, sodium borohydride, triphosgene, Hünig's reagent (DIEA), citric acid, sodium methoxide (MeONa), and Amberlite IR-120 plus (H⁺) were provided by Tokyo Chemical Industry Co., Ltd. (Shanghai, China). Hydrochloric acid (HCl), acetic acid (AcOH), anhydrous sodium sulfate (Na₂SO₄), sodium dihydrogen phosphate (NaH₂PO₄·2H₂O), sodium bicarbonate (NaHCO₃), dibasic sodium phosphate (Na₂HPO₄·12H₂O), tetrahydrofuran (THF), hexane, ethyl acetate (EtOAc), toluene, methanol (MeOH), acetonitrile, dichloromethane (DCM), ethanol (EtOH), trichloro-methane (CHCl₃), isopropanol (i-PrOH), and deuterated chloroform (CDCl₃) were supplied by Aladdin Chemistry Co. Ltd. (Shanghai, China).

β -gal, glutathione (GSH), hydrogen peroxide (H₂O₂), α -gal, reductase, phosphatase, cellulase, lysozyme, cysteine, hydrogen sulfide (H₂S), and dimethyl sulfoxide (DMSO, molecular biology grade) were bought from Sangon Biotech Co., Ltd. (Shanghai, China).

The absorption spectrum was measured using a Shimadzu UV-1800 spectrometer (Kyoto, Japan). Fluorescence emission spectrum was collected using a microplate reader (Infinite M200 PRO; TECAN, Switzerland).

DCMCA- β gal synthesis

DCMCA- β gal and other related intermediates were synthesized according to Scheme 1B and Scheme S1, specific details of the synthesis processes were provided in the supporting materials.

Incubation and determination system

The optical spectra of DCMCA- β -gal in reaction with β -gal were obtained at 37 °C in phosphate buffer saline (PBS, 0.1 M, pH=7.4, 30% DMSO). The fluorescence spectra were collected over a wavelength range of 500 – 800 nm after excitation at 464 nm. The selectivity of DCMCA- β gal for β -gal was evaluated with various interferences (100 equiv.) in our incubation system including GSH, H₂S, H₂O₂, cysteine, lysozyme, reductase, phosphatase, α -gal, and cellulase.

Cell culture and imaging

Human embryonic kidney cells (293T cells) and SKOV3 cells were provided by Shanghai Institutes of Biological Science, CAS (Shanghai, China). The 293T and SKOV3 cells were grown at 37 °C, 5% CO₂ in Dulbecco's modified Eagle's medium (DMEM) and McCoy's 5A Medium, respectively. The cytotoxicity of DCMCA- β gal towards 293T and SKOV3 cells was assessed by a colorimetric assay (MTT based). The cells were plated in a 96-well plate containing DMEM, and then different concentrations of DCMCA- β gal (containing 0.1% DMSO) were added. The absorbance of each well was recorded after 24 h of incubation.

For fluorescent imaging, the cells were incubated at 37 °C with DMEM and DCMCA- β gal (5 μ M) for 30 min. As a negative control, SKOV3 cells were also pretreated with the β -gal competitive inhibitor (D-galactose, 1 mM) for 1 h. Fluorescence

imaging and image collection were performed using a fluorescent microscope (BX53, Olympus, Japan).

In vivo imaging of β -gal activity

We created two ovarian cancer mouse models with SKOV3 cells. One was that, 1×10^7 SKOV3 and control 293T cells were subcutaneously inoculated into the right and left flanks of 7–8-week-old female nude mice, respectively; and the other was that SKOV3 cells were intraperitoneally injected into mice. Tumor-bearing mice of two models were both raised for approximately 10 days. In vivo fluorescence imaging was performed using the IVIS imaging system (PerkinElmer, USA), following intratumoral and intraperitoneal injection of 0.067 mg kg^{-1} DCMCA- β gal. Fluorescence imaging of the tumor tissues was conducted using a fluorescent microscope (BX53, Olympus, Japan), after sacrificing tumor-bearing mice 24 h post-DCMCA- β gal injection. All animal experiments were performed according to the protocol approved by the Animal Ethics Committee of East China Normal University (Permit Number: m20191005).

Conclusions

Here, we reported a sensitive β -gal activatable probe (DCMCA- β gal) for near-infrared imaging of ovarian tumors. The addition of β -gal to DCMCA- β gal generated significant fluorescence enhancement at approximately 680 nm, due to the generation of DCM-NH₂, a controllable NIR emission reporter. DCMCA- β gal possessed the advantages of high sensitivity, good photostability in dynamic living systems, and a larger spectral shift, which performed well in visualizing β -gal activity in SKOV3 human ovarian cancer cells and real-time imaging of β -gal activity in ovarian cancer mouse models. This study confirmed that DCMCA- β gal could provide an accessible tool for tracking β -gal activity in vivo and thereby imaging of ovarian tumors, which provides great preclinical potential for early diagnosis and therapy of ovarian cancer.

Conflicts of interest

There are no conflicts to declare.

Acknowledgements

This work was supported by the Key Project of Science and Technology Commission of Shanghai Municipality [grant number 18DZ1112700] and the National Natural Science Foundation of China [grant number 21675053].

Notes and references

- N. Thomakos, M. Diakosavvas, N. Machairiotis, Z. Fasoulakis, P. Zarogoulidis and A. Rodolakis, *Cancers (Basel)*, 2019, **11**, 1044-1060.
- P. Jessmon, T. Boulanger, W. Zhou and P. Patwardhan, *Expert Rev. Anticancer Ther.*, 2017, **17**, 427-437.
- L. Zhang, D. Pu, D. Liu, Y. Wang, W. Luo, H. Tang, Y. Huang and W. Li, *Lung Cancer*, 2019, **135**, 130-137.
- S. K. Chatterjee, M. Bhattacharya and J. J. Barlow, *Cancers Res*, 1979, **39**, 1943-1951.
- D. J. Spergel, U. Kruth, D. R. Shimshek, R. Sprengel and P. H. Seeburg, *Progress in Neurobiology*, 2001, **63**, 673-686.
- D. Asanuma, M. Sakabe, M. Kamiya, K. Yamamoto, J. Hiratake, M. Ogawa, N. Kosaka, P. L. Choyke, T. Nagano, H. Kobayashi and Y. Urano, *Nat Commun*, 2015, **6**, 6463-6469.
- H. M. Burke, T. Gunnlaugsson and E. M. Scanlan, *Chem Commun (Camb)*, 2015, **51**, 10576-10588.
- M. Sakabe, D. Asanuma, M. Kamiya, R. J. Iwatate, K. Hanaoka, T. Terai, T. Nagano and Y. Urano, *J Am Chem Soc*, 2013, **135**, 409-414.
- C. H. Tung, Q. Zeng, K. Shah, D. E. Kim, D. Schellingerhout and R. Weissleder, *Cancer Res*, 2004, **64**, 1579-1583.
- S. Wang, L. Chen, P. Jangili, A. Sharma, W. Li, J. Hou, C. Qin, J. Yoon and J. S. Kim, *Coord. Chem. Rev.*, 2018, **374**, 36-54.
- H. Wei, G. Wu, X. Tian and Z. Liu, *Future Med Chem*, 2018, **10**, 2729-2744.
- H. M. Kim and B. R. Cho, *Chem Rev*, 2015, **115**, 5014-5055.
- H. W. Liu, L. Chen, C. Xu, Z. Li, H. Zhang, X. B. Zhang and W. Tan, *Chem Soc Rev*, 2018, **47**, 7140-7180.
- Z. Yang, J. Cao, Y. He, J. H. Yang, T. Y. Kim, X. Peng and J. S. Kim, *Chem Soc Rev* 2014, **43**, 4563-4601.
- M. Kamiya, D. Asanuma, E. Kuranaga, A. Takeishi, M. Sakabe, M. Miura, T. Nagano and Y. Urano, *J Am Chem Soc*, 2011, **133**, 12960-12963.
- H. W. Lee, C. H. Heo, D. Sen, H. O. Byun, I. H. Kwak, G. Yoon and H. M. Kim, *Anal Chem*, 2014, **86**, 10001-10005.
- Z. Li, M. Ren, L. Wang, L. Dai and W. Lin, *Journal of Materials Chemistry B*, 2019, **7**, 3431-3437.
- K. Gu, Y. Xu, H. Li, Z. Guo, S. Zhu, S. Zhu, P. Shi, T. D. James, H. Tian and W. H. Zhu, *J Am Chem Soc*, 2016, **138**, 5334-5340.
- X. X. Zhang, H. Wu, 17P. Li, Z. J. Qu, M. Q. Tan and K. L. Han, *Chem Commun (Camb)*, 2016, **52**, 8283-8286.
- E. J. Kim, R. Kumar, A. Sharma, B. Yoon, H. M. Kim, H. Lee, K. S. Hong and J. S. Kim, *Biomaterials*, 2017, **122**, 83-90.
- B. Lozano-Torres, I. Galiana, M. Rovira, E. Garrido, S. Chaib, A. Bernardos, D. Munoz-Espin, M. Serrano, R. Martinez-Manez and F. Sancenon, *J Am Chem Soc*, 2017, **139**, 8808-8811.
- L. Peng, M. Gao, X. Cai, R. Zhang, K. Li, G. Feng, A. Tong and B. Liu, *J Mater Chem B*, 2015, **3**, 9168-9172.
- J. Zhang, P. Cheng and K. Pu, *Bioconjug Chem*, 2019, **30**, 2089-2101.
- Z. Li, M. Ren, L. Wang, L. Dai and W. Lin, *Sensors and Actuators B: Chemical*, 2020, **307**, 127643.
- X. Chen, X. Ma, Y. Zhang, G. Gao, J. Liu, X. Zhang, M. Wang and S. Hou, *Anal Chim Acta*, 2018, **1033**, 193-198.
- W. Wang, K. Vellaisamy, G. Li, C. Wu, C. N. Ko, C. H. Leung and D. L. Ma, *Anal Chem*, 2017, **89**, 11679-11684.
- X. Li, W. Qiu, J. Li, X. Chen, Y. Hu, Y. Gao, D. Shi, X. Li, H. Lin, Z. Hu, G. Dong, C. Sheng, B. Jiang, C. Xia, C.-Y. Kim, Y. Guo and J. Li, *Chemical science*, 2020, **11**, 7292-7301.
- W. Yang, B. Ling, B. Hu, H. Yin, J. Mao and P. J. Walsh, *Angew Chem Int Ed Engl*, 2020, **59**, 2.

ARTICLE

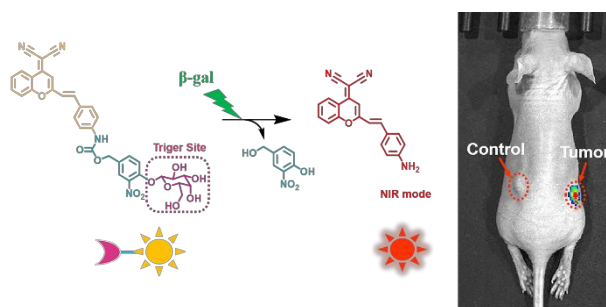
Journal Name

- 29 L. M. Lilley, S. Kamper, M. Caldwell, Z. K. Chia, D. Ballweg, L. Vistain, J. Krimmel, T. A. Mills, K. MacRenaris, P. Lee, E. A. Waters and T. J. Meade, *Angew Chem Int Ed Engl.*, 2020, **59**, 388–394.
- 30 W. Pham, Y. Choi, R. Weissleder and C. H. Tung, *Bioconjugate Chem*, 2004, **15**, 1403–1407.
- 31 L. Yuan, W. Lin, K. Zheng, L. He and W. Huang, *Chem Soc Rev*, 2013, **42**, 622–661.
- 32 Z. Guo, S. Park, J. Yoon and I. Shin, *Chem Soc Rev*, 2014, **43**, 16–29.
- 33 Z. Guo, W. Zhu and H. Tian, *Chem Commun (Camb)*, 2012, **48**, 6073–6084.
- 34 X. Wu, X. Sun, Z. Guo, J. Tang, Y. Shen, T. D. James, H. Tian and W. Zhu, *J Am Chem Soc*, 2014, **136**, 3579–3588.
- 35 W. E. Winter, 3rd, G. L. Maxwell, C. Tian, J. W. Carlson, R. F. Ozols, P. G. Rose, M. Markman, D. K. Armstrong, F. Muggia, W. P. McGuire and S. Gynecologic Oncology Group, *J Clin Oncol*, 2007, **25**, 3621–3627.
- 36 W. E. Winter, 3rd, G. L. Maxwell, C. Tian, M. J. Sundborg, G. S. Rose, P. G. Rose, S. C. Rubin, F. Muggia, W. P. McGuire and G. Gynecologic Oncology, *J Clin Oncol*, 2008, **26**, 83–89.
- 37 C. H. Tung, Q. Zeng, K. Shah, D. E. Kim, D. Schellingerhout and R. Weissleder, *Cancer Res*, 2004, **64**, 1579–1583.
- 38 Y. Urano, M. Kamiya, K. Kanda, T. Ueno, K. Hirose and T. Nagano *J Am Chem Soc*, 2005, **127**, 4888–4894.

View Article Online
DOI: 10.1039/D0TB02269A

Journal of Materials Chemistry B Accepted Manuscript

Graphical abstract



A sensitive fluorescent probe for β -galactosidase activity detection in vivo and near-infrared imaging ovarian tumors by detecting β -gal.